Lawrence Berkeley National Laboratory

Title
Balancing ion parameters and fluorocarbon chemical reactants for SiO2 pattern transfer control using fluorocarbon-based atomic layer etching

Authors
Dallorto, Stefano
Lorenzon, Monica
Szornel, Julia
et al.

Balancing ion parameters and fluorocarbon chemical reactants for SiO$_2$ pattern transfer control using fluorocarbon-based atomic layer etching

Stefano Dallorto, Monica Lorenzon, Julia Szornel, Adam Schwartzberg, Andy Goodyear, Mike Cooke, Martin Hofmann, Ivo W. Rangelow, and Stefano Cabrini

ARTICLES YOU MAY BE INTERESTED IN

Overview of atomic layer etching in the semiconductor industry
Journal of Vacuum Science & Technology A **33**, 020802 (2015); https://doi.org/10.1116/1.4913379

Surface prefunctionalization of SiO$_2$ to modify the etch per cycle during plasma-assisted atomic layer etching
Journal of Vacuum Science & Technology A **37**, 051003 (2019); https://doi.org/10.1116/1.5110907

Quasi-atomic layer etching of silicon nitride
Journal of Vacuum Science & Technology A **35**, 01A102 (2017); https://doi.org/10.1116/1.4967236

Fluorocarbon based atomic layer etching of Si$_3$N$_4$ and etching selectivity of SiO$_2$ over Si$_3$N$_4$
Journal of Vacuum Science & Technology A **34**, 041307 (2016); https://doi.org/10.1116/1.4954961

Predicting synergy in atomic layer etching
Journal of Vacuum Science & Technology A **35**, 05C302 (2017); https://doi.org/10.1116/1.4979019

Plasma etching of high aspect ratio features in SiO$_2$ using Ar/C$_4$F$_8$/O$_2$ mixtures: A computational investigation
Journal of Vacuum Science & Technology A **37**, 031304 (2019); https://doi.org/10.1116/1.5090606

Balancing ion parameters and fluorocarbon chemical reactants for SiO₂ pattern transfer control using fluorocarbon-based atomic layer etching

Stefano Dallorto,[1,2,3,a)] Monica Lorenzon,[1] Julia Szornel,[1] Adam Schwartzberg,[2]
Andy Goodyear,[3] Mike Cooke,[3] Martin Hofmann,[2] Ivo W. Rangelow,[2] and Stefano Cabrini[1]

[1]*Molecular Foundry, Lawrence Berkeley National Laboratory, Berkeley, California 94720*
[2]*Department of Micro- and Nanoelectronic Systems, Ilmenau University of Technology, 98684 Ilmenau, Germany*
[3]*Oxford Instruments Plasma Technology, North End, Yatton, Bristol BS49 4AP, United Kingdom*

In manufacturing, etch profiles play a significant role in device patterning. Here, the authors present a study of the evolution of etch profiles of nanopatterned silicon oxide using a chromium hard mask and a CHF₃/Ar atomic layer etching in a conventional inductively coupled plasma tool. The authors show the effect of substrate electrode temperature, chamber pressure, and electrode forward power on the etch profile evolution of nanopatterned silicon oxide. Chamber pressure has an especially significant role, with lower pressure leading to lower etch rates and higher pattern fidelity. The authors also find that at higher electrode forward power, the physical component of etching increases and more anisotropic etching is achieved. By carefully tuning the process parameters, the authors are able to find the best conditions to achieve aspect-ratio independent etching and high fidelity patterning, with an average sidewall angle of 87° ± 1.5° and undercut values as low as 3.7 ± 0.5% for five trench sizes ranging from 150 to 30 nm. Furthermore, they provide some guidelines to understand the impact of plasma parameters on plasma ion distribution and thus on the atomic layer etching process. *Published by the AVS.* https://doi.org/10.1116/1.5120414

I. INTRODUCTION

The demand for atomic-scale surface engineering and process controllability in advanced manufacturing and technologies has grown steadily in the latest years.[1] Critical dimensions and required pitch shrinkage call for increasingly higher etching precision and selectivity,[2–5] with the additional need for developing new processes to accommodate the increasing complexity in device structures.[6] Atomic layer etching (ALE) offers unmatched levels of control for etching performances, as required by the new technology node, and holds a great deal of potential to confront and overcome the challenges in modern nanofabrication techniques.[7]

In plasma-enhanced ALE, an inert plasma is typically maintained throughout, while alternating cycles of a reaction chemistry step, with a pulsed injection of precursors, and an etch step, when increased ion energy is applied to the wafer.[8,9] A fluorocarbon (FC) chemistry is used to deposit Angstrom-thick layers on SiO₂ to provide the reactant adsorption. A thin fluorinated SiO₂ surface layer (mixed layer) is then formed. Subsequently, low energy Ar ion bombardment is used to remove both the FC layer and the mixed layer. When Ar ions have energies below the threshold for SiO₂ physical sputtering, the etching is stopped right after the mixed layer has been removed;[10] ergo ALE is a self-limiting process.[11] To realize the FC layer deposition, we use pulsed CHF₃ injections into unbiased Ar plasma.[12] Keeping the substrate unbiased is integral to achieve a precise FC film thickness control, in the range of one to few Angstroms. Following FC deposition, a small forward bias plasma power [radio frequency (RF) power] is applied for 60 s. Powered electrodes cause the Ar ions to accelerate toward SiO₂ with maximum ion energies below the energy threshold for physical sputtering of unmodified SiO₂. At the end of a cycle, the process sequence is repeated to achieve precise control over the total etched thickness.

Despite the benefits of atomic layer etching, few demonstrations in patterning of SiO₂ using CHF₃/Ar plasma have been reported. In this work, our main goal is the optimization of the SiO₂ etching profile for nanoscale-size features (30–200 nm), which we tackle by investigating the effect of each plasma parameter on the whole ALE process. Such an in-depth study allows us to critically identify the extent of each parameter's impact and therefore to design the ideal process to obtain nanoscale-sized, aspect-ratio independent features. Moreover, the thorough understanding of the effect of parameters such as the substrate temperature, pressure, and forward bias power on the etched profiles enables an indirect feedback loop that allows us to infer the plasma parameters by evaluating the resulting etched features.

In a previous study,[13] we reported the first demonstration of aspect-ratio independent ALE and the achievement of the theoretically predicted self-limiting behavior and therefore provided a guideline recipe for an optimized SiO₂ patterning at the nanoscale level (down to 30 nm feature size). In addition, we showed the synergy of the ALE process: the combination

---

of the FC deposition step and the Ar etch step causes SiO_2 etching. We developed our process in a conventional inductively coupled plasma (ICP) tool, which provides the additional benefit of enabling a cost-effective process and straightforward transfer to scale production protocols in the manufacturing industry.

Here, we present the profile evolution of silicon oxide using a Cr hard mask and we extend our previous investigation by performing a detailed and systematic analysis to gain a better insight into the effect of each parameter on the overall etching process. To this aim, we conduct a series of experiments in which we tune one parameter at a time, while the others are kept at the optimized values of the standard recipe,[13] with the focus on high fidelity transfer and vertical sidewalls fabrication. Our main findings are (i) an intermediate temperature (T = −10 °C) allows for slow deposition rates, directional transfer (and therefore vertical sidewalls), and flat bottom surfaces; (ii) the profile is further improved by working at very low pressure (p = 5 mTorr), since the ion energy is higher and the concentration of radicals is low, which makes the anisotropic etching by Ar ions the dominant process and leads to vertical features with limited undercut; and (iii) higher forward bias power (P_{Bias} = 4W) significantly increases the directionality of the ion bombardment and therefore improves the verticality of the etching profile. Combining the best parameters into one process, we demonstrate the achievement of high fidelity transfer and aspect-ratio independent etching (ARIE) via ALE, with features exhibiting average undercut values as low as $3.7 \pm 0.5\%$ for five trench sizes, from 150 to 30 nm, as well as an average sidewall angle of $87° \pm 1.5°$, very close to the $90°$ value of an ideal, perpendicular wall.

II. EXPERIMENT

A. Cr mask patterning

For the patterning of the Cr hard mask, a lift-off process has been used. First, nano-sized lines are created on poly(methyl methacrylate) (PMMA) using electron-beam lithography (Vistec VB300) on wafers with Si substrates with 250 nm of thermally grown SiO_2. The PMMA thickness is 60 nm, and the line width varies from 30 to 200 nm. Next, a 12 nm chromium (Cr) layer at a pressure of 2×10^{-6} Torr is formed using e-beam evaporation. A final lift-off process with Remover PG (MicroChem) followed by acetone cleaning in an ultrasonic bath is used to define the Cr lines.

B. Atomic layer etching

Atomic layer etching is carried out in a conventional Plasmalab System 100 ICP etcher from Oxford Instruments Plasma Technology with liquid nitrogen cryogenically cooled staged. Forward RF power (13.56 MHz) is applied to the substrate electrode to accelerate ions toward the substrate. The samples are cut and bonded onto 4 in. silicon carried wafers using Fomblin oil, which improves the thermal contact between the sample and the carrier.
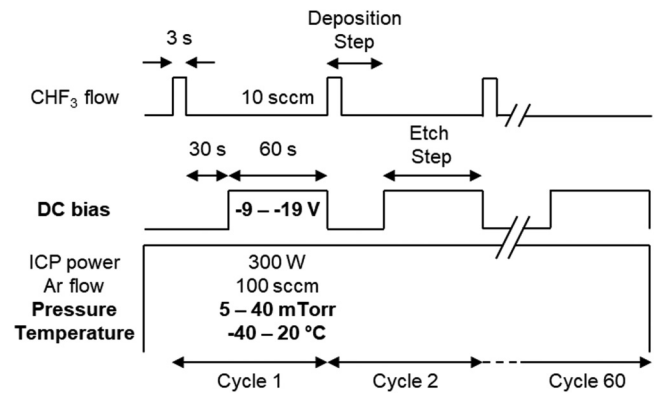

FIG. 1. Schematic of the cyclic ALE process used, consisting of a repeating deposition step and etch step. The process parameters which we vary are the substrate temperature, the forward bias power, and the process pressure.

Figure 1 shows a schematic ALE process sequence. Ar gas is flowed continuously at 100 sccm during the entire process. The ICP power is held constant at 300 W, which creates a steady state Ar plasma for the entire length of the process. For the deposition half-cycles, short periodical injections of 10 sccm of CHF_3 are introduced. The injection time is 3 s to ensure a stable and reproducible FC injection. After the CHF_3 pulse, a purging step of 30 s with pure Ar plasma ensures that all the FC compounds are exhausted from the process chamber. The forward bias power supplied by the substrate electrode generates a direct current (DC) bias that controls the ion energy at the substrate. The deposition and purge steps are unbiased (DC bias = 0 V). During the etch half-cycle, forward RF power is applied (P_{Bias} = 2–4 W) to generate a DC bias in the range of −9 to −19 V. The etch step length is fixed at 60 s. Forward bias power (DC bias), pressure, and substrate temperature are varied to investigate a wide range of parameters. Etched samples are imaged in a Zeiss Ultra 60 scanning electron microscope (SEM) to determine the SiO_2 profile and depth. FC polymer deposition is also measured on blank SiO_2 wafers using a UVISEL spectroscopic ellipsometer from Horiba.

The ion energy distribution (IED) of the plasma is measured using a commercial retarding field energy analyzer Semion™ System 500.[14,15] IED is collected as a function of the pressure, using pure Ar plasma with 300 W inductively coupled source power and 2 W forward bias power.

III. RESULTS AND DISCUSSION

In this work, we aim to target the optimization of the SiO_2 etching profile for nanoscale-size features (30–200 nm) by means of investigating the effect of parameters such as the temperature, pressure, and forward bias power on the etched profiles.

We then evaluate their impact on the etched features by comparing key profile parameters, namely, the sidewall angle (ϑ), the undercut, and the etching rate per cycle (EPC, Å/cycles), as depicted in Fig. 2. The sidewall angle ϑ describes the deviation from an ideal, perpendicular sidewall and is defined as the angle that the lateral wall forms with the plane
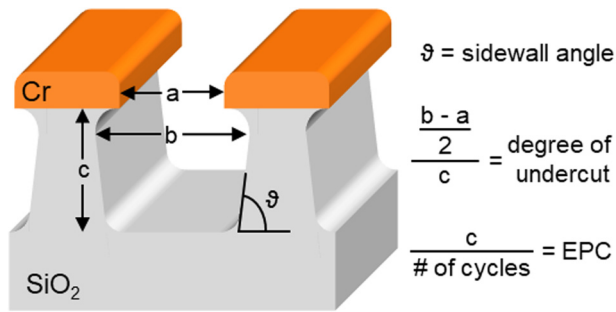
FIG. 2. Schematic cross section of samples used in this work with features parameter definition: sidewall angle, degree of undercut, and etching per cycle (EPC).

tangent to the surface, with 0° being parallel to such surface and 90° representing the ideal, perpendicular sidewall. The undercut percentage measures the amount of SiO_2 that has been removed from the region underlying the Cr mask, thus introducing a deviation from the ideal pattern transfer and causing the lateral walls to form the sidewall angle ϑ. We calculate the degree of undercut as $(((b-a)/2)/c) \cdot 100$, i.e., the difference between the widest (b) and narrowest (a) widths of the feature after etching is completed, normalized to the thickness of the SiO_2 etched feature (c). An undercut close to 0 and a sidewall angle reaching 90° describe the achievement of high fidelity pattern transfer. Finally, we define the etching depth of each cycle (EPC, Å/cycle) as the

thickness of the SiO_2 etched feature (c) divided by the total number of cycles, which is 60 for all the etching processes reported in this work.

We measure and report these parameters (sidewall angle, undercut, and EPC) as a function of the substrate temperature, the process pressure, and the forward bias power. The plotted trends consist of the average values between different trench sizes (30, 40, 50, 100, 150, and 200 nm), with the respective error bars computed as the standard deviation from each average.

A. Effect of the substrate temperature on ALE mechanism

We start our investigation with a detailed analysis of the temperature effect on the SiO_2 etch profile, reported in Fig. 3. As noticed in our previous work,[13] the substrate temperature has a non-negligible impact on the ALE performances, since it strongly affects the sticking coefficient of the deposited FC polymer and therefore the overall ALE process.[16] In addition, the temperature also has a significant effect on the chemical etching caused by fluorine in the chamber. When the substrate temperatures are higher than $T = -10\,°C$, the etching rate increases, due to residual fluorine radicals coming from the chamber wall. Moreover, higher temperatures ($T = -10\,°C$ to $+20\,°C$) enhance SiO_2 chemical etching by fluorine, generating an undesired reaction between the FC polymer and the SiO_2 surface during each ALE cycle.[17] Increasing the

FIG. 3. (a) Cross-sectional SEM images of silicon oxide features patterned using FC-Ar ALE, reported for three different processing temperatures, namely, $T = 20\,°C$ (top panel), $T = -10\,°C$ (center), and $T = -40\,°C$ (bottom panel). Two different trench sizes are shown: 40 and 150 nm. Both features for each temperature are obtained after 60 ALE cycles. The scale bar is 40 nm for all panels. (b) Etched silicon oxide thickness per cycle (EPC, Å/cycle, black dots, left axis) and fluorocarbon film thickness per cycle (orange squares, right axis) deposited onto SiO_2 during one ALE cycle. Both are reported as a function of the substrate temperature during the process. (c) Sidewall angle (black dots, left axis) and degree of undercut (blue squares, right axis) as a function of the substrate temperature.

chemical reaction between SiO_2 and FC results in a higher etch rate, but at the expense of the film integrity and etch selectivity for SiO_2 over other materials.[18–20] However, while we demonstrated that ALE at $T = -10\,°C$ ensures self-limiting behavior and aspect-ratio independent etching,[13,21,22] to date, no study has been reported on the temperature effect on the ALE patterning of silicon oxide.

Here, we perform ALE at three different temperatures: $T = -40$, -10, and $+20\,°C$. Figure 3(a) shows the corresponding SEM pictures for 40 and 150 nm trenches. We kept the pressure and forward bias power at fixed values, respectively, $p = 10\,mTorr$ and $P_{Bias} = 2W$, which corresponds to a DC bias of $-9\,V$. EPC, sidewall angle, and undercut are displayed in Figs. 3(b) and 3(c). Although the EPC remains constant throughout the investigated temperature range, the deposition per cycle drops from 7 Å/cycle at $T = -40\,°C$ to 3 Å/cycle at $T = +20\,°C$. The detrimental effect of a higher FC deposition rate is particularly evident by looking at the bottom of the 150 nm features. Such round surfaces become more and more flat with increasing temperatures, as can be appreciated in the flat bottom of the same size feature (150 nm) for $T = +20\,°C$. Moreover, the bottom of the features obtained at $T = -40\,°C$ also exhibits increased roughness, which indicates incomplete removal of the FC polymer. This effect stems from the fact that the lower temperature leads to thicker FC films, which requires longer etching steps in order to completely remove both the FC and mixed layers. On the other hand, the flat surface obtained at $T = +20\,°C$ is accompanied by a higher undercut value and a more inclined sidewall [see data in Fig. 3(c)], whereas such values are slightly improved for a substrate temperature of $T = -10\,°C$. As a result, we identify the latter value as the best compromise within the probed temperature range between a slow deposition rate and an optimal directional transfer, in order to obtain improvements in both flat bottom surfaces and vertical features.

Importantly, our data allow us to draw important conclusions on the ALE mechanism. We show that ALE etching of SiO_2 strongly depends on the synergy between the accelerated Ar ions and the FC layer, while being softly sensitive to the range of temperatures we explore ($T = -40$ to $+20\,°C$). Hence, ALE does not operate as a thermally activated process, but rather finds its dominant driving force in a combination of chemical and kinetic processes between the accelerated ions and the mixed layer.

B. Effect of the pressure and ion energy distribution

Pressure is another pivotal parameter in ALE, since it directly affects the Ar ions flux and energy, as well as the concentration of Ar, C, and F radicals in the plasma. In order to study the effect of pressure alone, we maintain a fixed substrate temperature of $T = -10\,°C$ and forward bias power at $P_{Bias} = 2\,W$ (DC bias of $-9\,V$) and we change the pressure level from $p = 5\,mTorr$ to $p = 10$, 25, and 40 mTorr to conduct the ALE process, as reported in Fig. 4(a). During each experiment, the pressure is kept

constant thanks to the automatic pressure controller of our Plasmalab System 100 ICP.

In order to gain better insight into the process mechanisms, for each pressure level we carefully characterize the IED of the Ar plasma, as shown in Fig. 4(b). The IED for the lowest pressure values (namely, $p = 5\,mTorr$ and $p = 10\,mTorr$) exhibits a single peaked energy distribution. Such a distinct peak corresponds to the average energy that the ions gain while traveling across the plasma sheath.[15] When the chamber pressure increases, the mean free path of the ions becomes shorter than the plasma sheath width. As a result, the ions will no longer travel ballistically through the sheath but will experience collisions with neutral gas molecules and radicals before striking the electrode. The collisions with the neutrally-charged particles cause ions to lose energy, which results in the IED shifting to lower values [see Fig. 4(b) for $p = 25\,mTorr$ and $p = 40\,mTorr$].[23]

The different IEDs at the various pressure levels directly affect the etching features. For instance, at low pressure ($p = 5\,mTorr$) the F and C radical densities are relatively low,[24] while the ion energy is the highest between the investigated pressure levels. As a result, the etching results into an anisotropic etching with a reduced EPC [see Fig. 4(c)] and a steep sidewall (86°) [Fig. 4(d)]. On the other hand, the SEM pictures [Fig. 4(a), 150 nm half-pitch, $p = 5\,mTorr$] highlight an increased roughness at the bottom of the trench, suggesting that the FC film cannot be completely removed by the ions during the etch step. In order to confirm this hypothesis, we perform additional experimentation with the same parameters but longer etch steps, i.e., the time interval has been increased from $t_{etch} = 60\,s$ to $t_{etch} = 180\,s$. As reported in Fig. 5, a longer etching time indeed allows for a complete removal of the polymer and leads to a flat bottom surface.

When the pressure increases, more radicals become available from the plasma system, and the etch rate grows by over 60% from a chamber pressure of $p = 5\,mTorr$ to $p = 40\,mTorr$. Concurrently, the features become more tapered and show a larger local bowing. The etching rate trend hints to the fact that at higher pressure we are working in a chemical-reaction limited regime, as opposed to a physical-reaction limited where the etch rate would decrease. The monotonic growth of the undercut confirms the chemical-limited regime, since an increased undercut is due to chemical etching by the F radicals. Finally, we note that the sidewall angle decreases with pressure with the best result obtained at $p = 5\,mTorr$ with an 86° angle. This is a further confirmation that a lower pressure enables anisotropic etching thanks to the combined effect of high ion energy and a lower contribution to the isotropic etching by the F radicals at a low concentration.

C. Effect of the bias power on the etching directionality

Finally, we examine the effect of the forward bias power and, consequently, of the DC bias on the etched profiles. All other parameters are kept constant, with a pressure of $p = 10\,mTorr$ and a temperature of $T = -10\,°C$, based on the
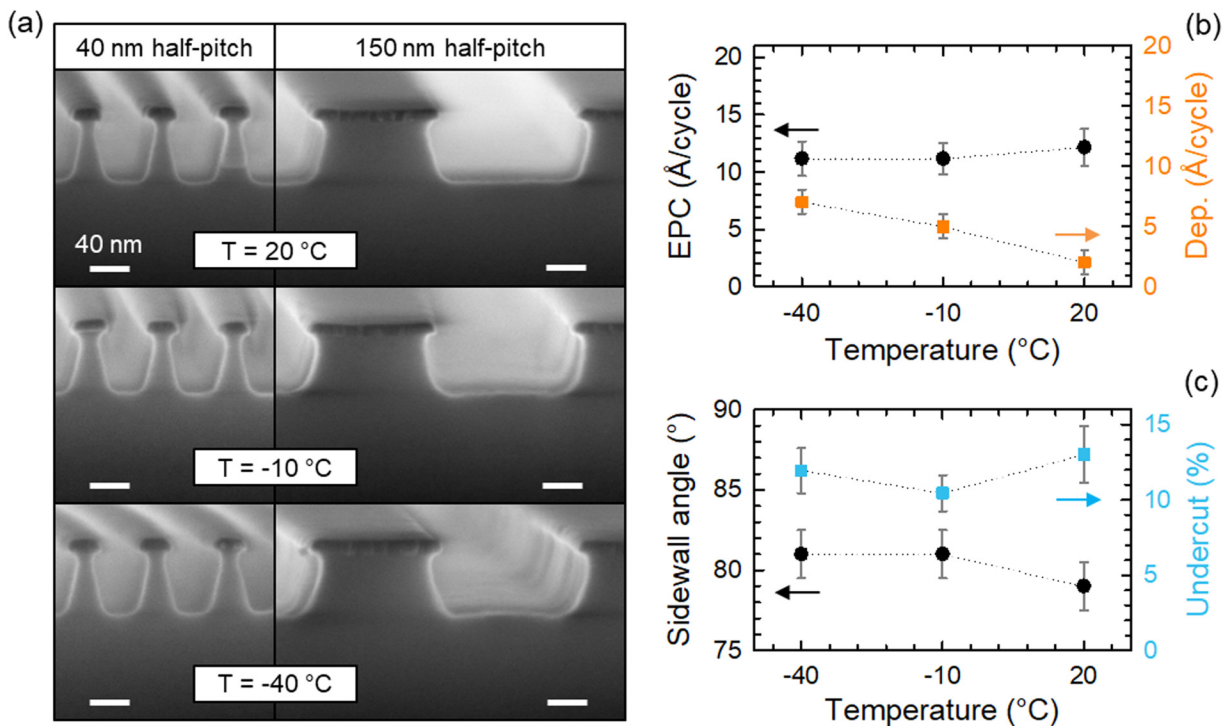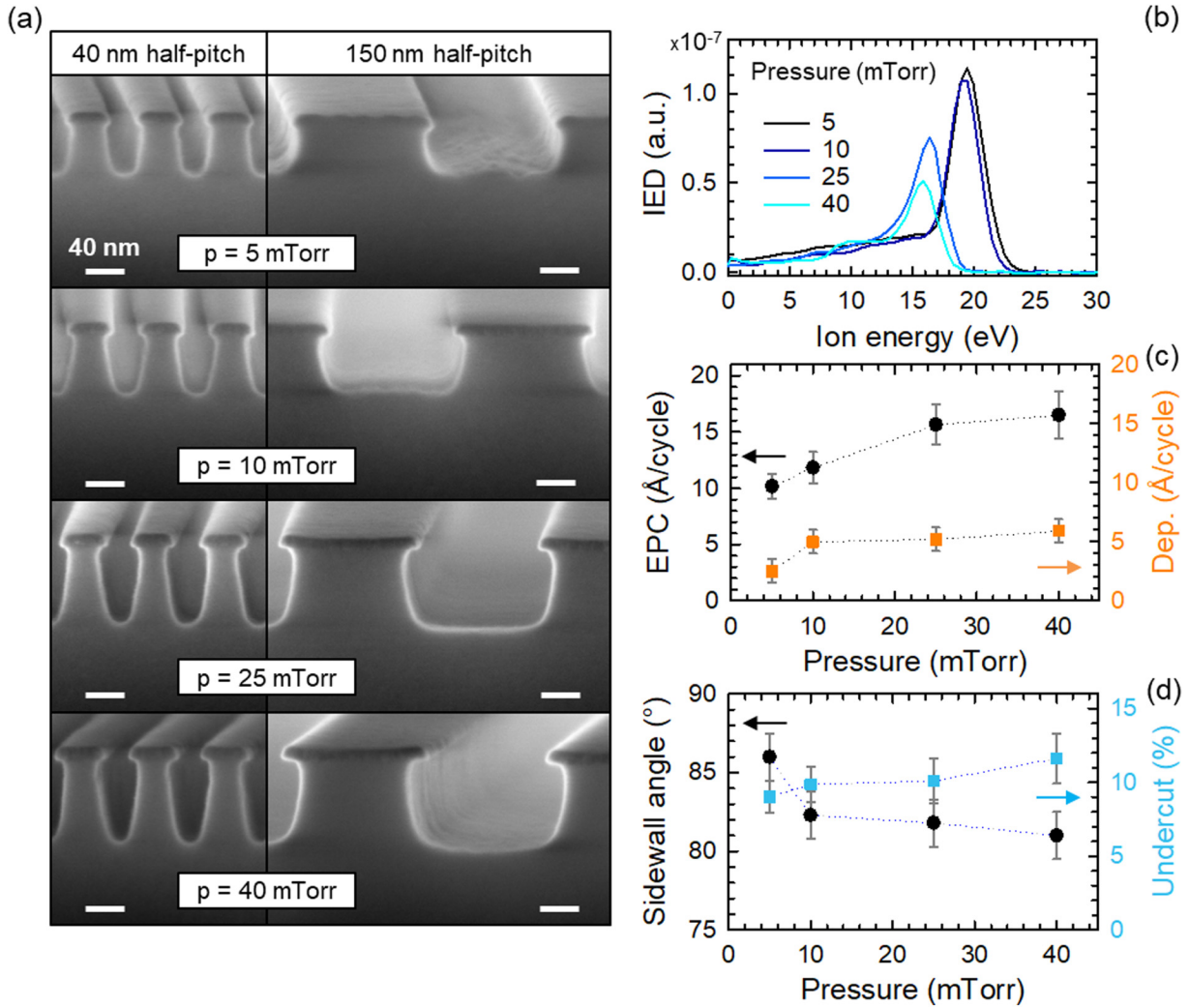
FIG. 4. (a) Cross-sectional SEM images of silicon oxide features patterned using FC-Ar ALE reported for four different pressure values, p = 5, 10, 25, and 40 mTorr. Two different trench sizes are shown: 40 and 150 nm. Both features for each pressure value are obtained after 60 ALE cycles. The scale bar is 40 nm for all panels. Etched silicon oxide thickness per cycle (EPC, Å/cycle, black dots, left axis) and fluorocarbon film thickness per cycle (orange squares, right axis) deposited onto SiO$_2$ during one ALE cycle. Both are reported as a function of the pressure values reported in (a). (c) Sidewall angle (black dots, left axis) and degree of undercut (blue squares, right axis) as a function of the pressure values in (a). (d) IED for each pressure value as in (a). The experimental parameters used to measure the IED are −9 V DC bias, 300 W ICP power, and 100 sccm Ar flow.

best results of our previous study which we know ensure a self-limiting behavior and aspect-ratio independent etching.[13]

The profile evolution of SiO$_2$ features is shown in Fig. 6(a) for increasing forward DC bias applied during the etch step. In order to work inside the ALE process window, and avoid any sputtering of SiO$_2$ during the etch step, the maximum DC bias allowed is −19 V.[11,13]

Figure 6(b) shows the etching rate trend as a function of the increasing negative bias, which corresponds to an increase in the forward bias power from P_{Bias} = 2 W (DC bias = −9 V) to P_{Bias} = 3 W (DC bias = −12 V) and P_{Bias} = 4 W (DC bias = −19 V). The deposition per cycle is not reported since it is a constant value of 5 Å/cycle for all the applied bias. Indeed, the FC deposition step in the ALE process is independent from the power applied during the etch step. Following the increase of the forward power, the Ar ion energy distribution shifts to larger values.[25,26] As a result, ions with a higher energy interact with the mixed layer during the etch step,

which leads to a deeper SiO$_2$ etching and higher EPC. Lower forward biases and therefore lower Ar ion energies have the additional, undesired effect of needing a longer time to completely remove the FC layer, causing an incomplete removal of the mixed layer at the bottom of the feature.

Another consequence of the increasing forward power is that more ions are incident on the electrode with a smaller deflection angle due to the smaller contribution of the ion-neutral scattering at higher energies.[27] This effect is appreciated in the sidewall angle and undercut trends shown in Fig. 6(c): the profiles become more vertical, with the angle increasing from 78° at −9 V DC bias to 85° at −19 V DC bias and the undercut dropping from 10% down to 6% for the same DC bias values, respectively.

We therefore reach the important conclusion that an increase in the forward power improves the overall feature shape, since it allows for a more anisotropic etching. In this case, the competition between FC deposition and ion bombardment leads to
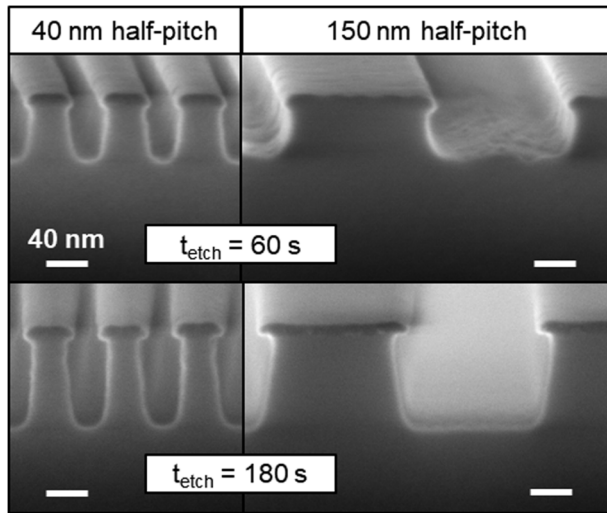
FIG. 5. Cross-sectional SEM images of silicon oxide features patterned using FC-Ar ALE reported for two different etch times: $t_{etch} = 60\,s$ and $t_{etch} = 180\,s$. Two different trench sizes are shown: 40 and 150 nm. Both features for each pressure value are obtained after 60 ALE cycles. The scale bar is 40 nm for all panels.

more vertical feature walls, a limited undercut, and a flat bottom of the features, therefore balancing the deposition and the etch step within one ALE cycle. We identify −19 V DC bias (corresponding to $P_{Bias} = 4\,W$) as the optimum value to use in future patterning design of SiO_2.

D. Aspect-ratio independent etching

Figures 7(a)–7(e) show a series of Cr masked SiO_2 features with different trench sizes, etched for 60 ALE cycles under the optimal ALE self-limiting conditions that we have gathered throughout this work for obtaining flat surfaces, namely, T = −10 °C, p = 5 mTorr, DC bias = −19 V, $t_{etch} = 60\,s$. Previously (Fig. 5), we show that for a pressure of 5 mTorr and DC bias=−9 V an etch time of 180 s is needed for completely removing the FC polymer. However, using a higher DC bias of −19 V allows for complete removal of the polymer after 60 s. Notably, all features exhibit the same vertical profile, with an average value of 87° ± 1.5°, very close to a perfectly perpendicular wall (90°), as well as a low undercut of 3.7 ± 0.5%, which demonstrate that our process allows for achieving ARIE in a conventional ICP tool.

Furthermore, features with large aspect ratios etch as fast as those with low aspect ratios, regardless of the feature width. A slight undercut beneath the mask can still be observed and can be ascribed to chemical and/or kinetic processes, such as ions and radicals reflected from the edges of the feature, broad Ar ions angular distribution, or residual fluorine from the chamber wall.[22] Conversely, we can rule out the contribution of ions scattered from the feature edges, since the sidewall profile does not change significantly with the feature width. On the basis of our previous[13] and present work, we can conclude that the main cause of the undercut is coming from the fluorine radicals in the chamber. Our study therefore
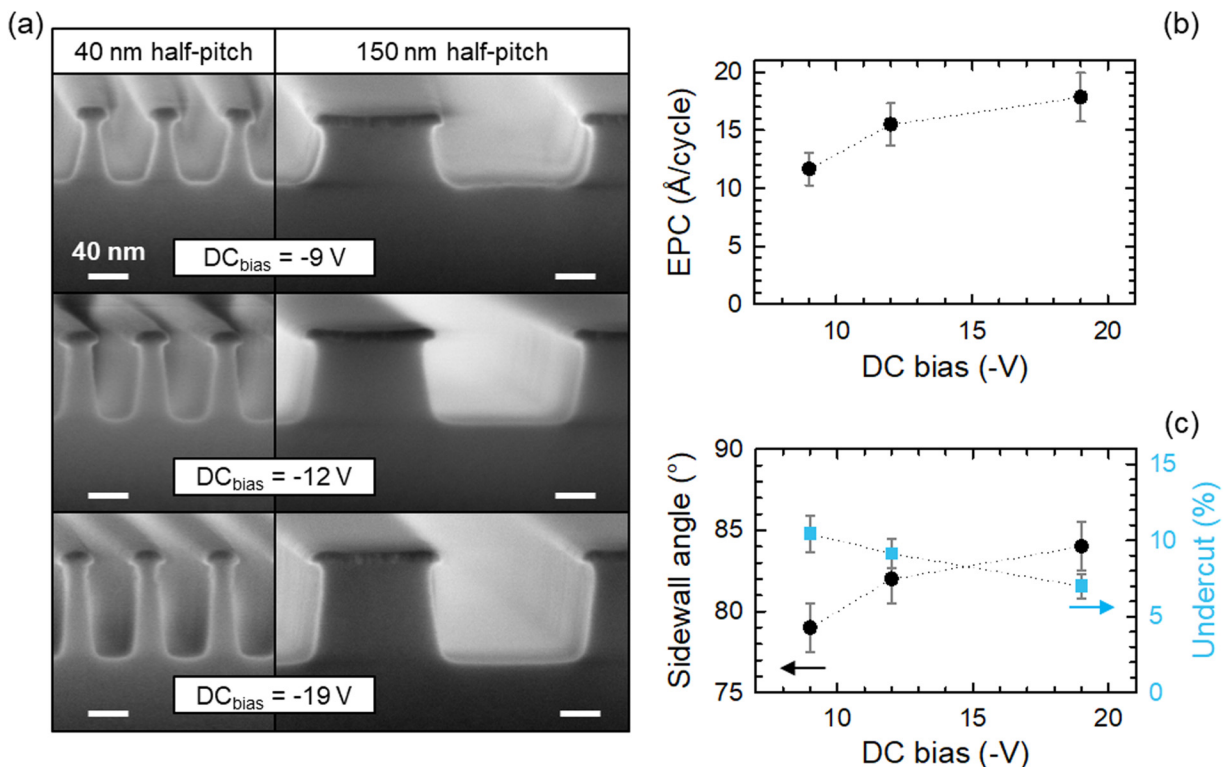

FIG. 6. (a) Cross-sectional SEM images of silicon oxide features patterned using FC-Ar ALE reported for three different forward bias power, namely, P = 2, 3, and 4 W, corresponding to an applied DC bias of −9, −12, and −19 V. Two different trench sizes are shown: 40 and 150 nm. Both features for each DC bias are obtained after 60 ALE cycles. The scale bar is 40 nm for all panels. (b) Etched silicon oxide thickness per cycle (EPC, Å/cycle, black dots) as a function of the same negative DC bias values reported in (a). (c) Sidewall angle (black dots, left axis) and degree of undercut (blue squares, right axis) as a function of the negative DC bias as in (a).
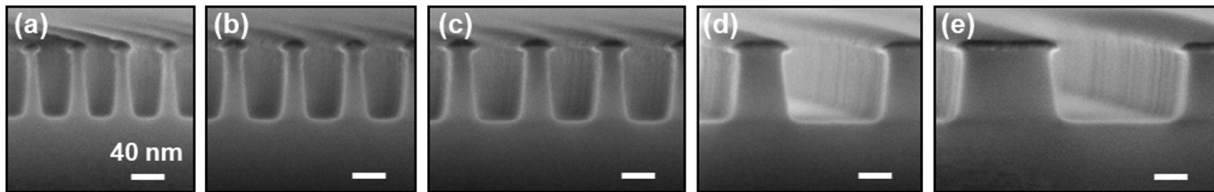
FIG. 7. (a)–(e) Cross-sectional SEM images of silicon oxide features patterned using FC-Ar ALE. Different trench sizes after 60 ALE cycles: 30, 40, 50, 100, and 150 nm from (a) to (e). Experimental parameters are T = −10 °C, p = 5 mTorr, DC bias = −19 V, and ICP power 300 W. The scale bar is 40 nm for all panels.

highlights that, in order to achieve features without any undercut and thus a complete ALE, it is paramount to find a careful balance between the Ar ion parameters (i.e., energy and angular distribution) and the FC chemical reactants.

IV. SUMMARY AND CONCLUSIONS

In this work, we extensively study and characterize a cyclic CHF_3/Ar ALE process using a conventional ICP tool. We investigate the effect that the main process parameters, namely, the substrate temperature, chamber pressure, and bias power, have on the etching of 30–150 nm features into SiO_2, in order to gain better insight into the ALE mechanism while simultaneously finding the best conditions for the ALE process.

We find that the investigated temperature range (T = −40 to +20 °C) does not have a significant effect on the ALE behavior, which helps us to draw the important conclusion that the ALE is not a thermally activated process, but rather is dominated by concurrent chemical and kinetic processes between the accelerated Ar ions and mixed layer. However, we can still identify T = −10 °C as the best compromise between a slow deposition rate and an ideal directional transfer, which allows for the realization of features with both a flat bottom surface and vertical lateral walls.

Conversely, the pressure has a more significant impact on the process, thanks to its direct effect on the ion energy distribution. Low pressure values (p = 5 mTorr) result in high ion energy and low density of F and C radicals, whose isotropic contribution to the etching thus becomes negligible. Hence, the anisotropic etching from the Ar ions dominates and enables the achievement of a reduced EPC and steep sidewalls (up to 86°). Such ideal, vertical features are counterbalanced by the negative effect of rough and round bottom surfaces, due to incomplete removal of the FC film at low pressure. However, we demonstrate that this issue can be easily overcome by increasing the etching time from t_{etch} = 60 s to t_{etch} = 180 s or increasing the bias voltage, thus allowing us to achieve flat bottom surfaces at low pressure values.

Etching directionality is also directly affected by the forward bias power, as shown through the exploration of three different bias powers (P_{Bias} = 2, 3, and 4 W, corresponding to DC bias of −9, −12, and −19 V). In this case, a higher forward power leads to an increase in the ion energy distribution and smaller deflection angle, which translates into a deeper etching, complete removal of the FC layer, and improved verticality of the etched features thanks to the dominant contribution of anisotropic over isotropic etching.

Combining the best parameter values that we find from the analysis of each parameter alone, that is, intermediate temperature (T = −10 °C), low pressure (p = 5 mTorr), and high forward bias power (P_{Bias} = 4 W), we demonstrate the achievement of etched features with exceptionally low undercut values (down to an average of 3.7 ± 0.5%, calculated from five features ranging from 150 to 30 nm), almost vertical sidewalls (87° ± 1.5°, very close to an ideal 90° perpendicular wall), flat bottom surfaces, and, importantly, aspect-ratio independent etching, which is extremely important for the actual integration of the ALE approach into existing production lines. Moreover, besides providing a paradigm process to obtain ARIE, our study fulfills the goal of gaining some important insight into the plasma physics and the mechanisms that drive the ALE process. We find that, while the thermal activation is a negligible effect, the driving force during ALE pattern transfer is a finely tuned balance between the kinetic and chemical reactions between the Ar ions and the FC radicals.

Finally, we notice that an accurate understanding of how each plasma parameter affects the ALE process enables a qualitative, but reliable feedback control on the plasma itself, since we learned how the etched features and their sidewall angle, undercut degree, and bottom surfaces carry information about whether they are generated by anisotropic/isotropic mechanisms (ions vs radicals) and either higher/lower temperature, pressure, and bias power.

[1]N. Marchack and J. P. Chang, J. Phys. D Appl. Phys. **44**, 174011 (2011).
[2]V. M. Donnelly and A. Kornblit, J. Vac. Sci. Technol. A **31**, 050825 (2013).
[3]M. Leskelä and M. Ritala, Angew. Chem. Int. Ed. **42**, 5548 (2003).
[4]C. G. Lee, K. J. Kanarik, and R. A. Gottscho, J. Phys. D Appl. Phys. **47**, 273001 (2014).
[5]S. Dallorto, D. Staaks, A. Schwartzberg, X. Yang, K. Y. Lee, I. W. Rangelow, S. Cabrini, and D. L. Olynick, Nanotechnology **29**, 405302 (2018).

[6]K. J. Kanarik, G. Kamarthy, and R. A. Gottscho, Solid State Technol. **55**, 15 (2012).

[7]K. J. Kanarik, S. Tan, and R. A. Gottscho, J. Phys. Chem. Lett. **9**, 4814 (2018).

[8]D. Metzler, C. Li, S. Engelmann, R. L. Bruce, E. A. Joseph, and G. S. Oehrlein, J. Vac. Sci. Technol. A **34**, 01B101 (2016).

[9]D. Metzler, R. L. Bruce, S. Engelmann, E. A. Joseph, and G. S. Oehrlein, J. Vac. Sci. Technol. A **32**, 020603 (2014).

[10]S. Rauf, T. Sparks, P. Ventzek, V. Smirnov, A. Stengach, K. Gaynullin, and V. Pavlovsky, J. Appl. Phys. **101**, 033308 (2007).

[11]G. Oehrlein, D. Metzler, and C. Li, ECS J. Solid State Sci. Technol. **4**, N5041 (2015).

[12]D. Metzler, C. Li, S. Engelmann, R. L. Bruce, E. A. Joseph, and G. S. Oehrlein, J. Chem. Phys. **146**, 052801 (2017).

[13]S. Dallorto, A. Goodyear, M. Cooke, J. E. Szornel, C. Ward, C. Kastl, A. Schwartzberg, I. W. Rangelow, and S. Cabrini, Plasma Process. Polym. 16, e1900051 (2019).

[14]D. Gahan, S. Daniels, C. Hayden, D. O'Sullivan, and M. Hopkins, Plasma Sources Sci. Technol. **21**, 015002 (2011).

[15]D. Gahan, B. Dolinaj, and M. Hopkins, Rev. Sci. Instrum. **79**, 033502 (2008).

[16]D. Metzler *et al.*, J. Vac. Sci. Technol. A **34**, 01B102 (2016).

[17]D. Flamm, C. Mogab, and E. Sklaver, J. Appl. Phys. **50**, 6211 (1979).

[18]K. H. Kirmse, A. E. Wendt, G. S. Oehrlein, and Y. Zhang, J. Vac. Sci. Technol. A **12**, 1287 (1994).

[19]M. Schaepkens and G. S. Oehrlein, J. Electrochem. Soc. **148**, C211 (2001).

[20]J. Butterbaugh, D. Gray, and H. Sawin, J. Vac. Sci. Technol. B**9**, 1461 (1991).

[21]S. Tachi, K. Tsujimoto, and S. Okudaira, Appl. Phys. Lett. **52**, 616 (1988).

[22]R. J. Gasvoda, A. W. van de Steeg, R. Bhowmick, E. A. Hudson, and S. Agarwal, ACS Appl. Mater. Interfaces **9**, 31067 (2017).

[23]R. Seeböck, W. Köhler, and M. Römheld, Contrib. Plasma Phys. **32**, 613 (1992).

[24]K. Maruyama, K. Ohkouchi, Y. Ohtsu, and T. Goto, Jpn. J. Appl. Phys. **33**, 4298 (1994).

[25]A. Agarwal and M. J. Kushner, J. Vac. Sci. Technol. A **27**, 37 (2009).

[26]C. M. Huard, S. Sriraman, A. Paterson, and M. J. Kushner, J. Vac. Sci. Technol. A **36**, 06B101 (2018).

[27]D. Q. Wen, Y. R. Zhang, M. A. Lieberman, and Y. N. Wang, Plasma Process. Polym. **14**, 1600100 (2017).